COMPUTER-AIDED DESIGN & APPLICATIONS, 2016
VOL. 13, NO. 4, 484–489
http://dx.doi.org/10.1080/16864360.2015.1131542

A new approach for irregular porous structure modeling based on centroidal Voronoi tessellation and B-spline

Y.H. You, S.T. Kou and S.T. Tan

The University of Hong Kong, Hong Kong

ABSTRACT

In this paper, we introduce a new approach for irregular porous structure modeling based on centroidal Voronoi tessellation (CVT) and B-Spline. Given an arbitrary domain, a CVT is first constructed on it, decomposing the domain into a set of Voronoi cells. A scaled Voronoi cell is then generated within each Voronoi cell of the CVT with respect to a unique scale factor. Finally, a pore is generated in each Voronoi cell by using B-Spline with the vertices of each scaled Voronoi cell being the control points. Compared to existing approaches, the proposed method is much more flexible to control the pore size and distribution both globally and locally. In addition, our method can effectively prevent overly large or small angles within Voronoi cells, which are the source of simulation errors and computational burdens in finite element analysis (FEA).

KEYWORDS

Irregular porous structure; centroidal Voronoi tessellation; B-spline; mesh quality

1. Introduction

Porous structure is a particular type of solid with pores. Different pore parameters, such as size, shape, porosity, and pore interconnection, lead to diverse porous structures. Compared to conventional solids, porous structures possess many superior properties including lower density, lower thermal conductivity, lower stiffness, lower strength, larger compressive strain and larger surface areas [13], [26]. In recent years, porous structures have been widely utilized into the areas of tissue engineering [12], energy absorbers [1], [25], thermal insulators [3], [24] and lightweight structures [7], [15].

The wide applications of porous structures have attracted a lot of attention on porous structure modeling. Computer-Aided Design (CAD) plays an important role in this research topic because of the easy manipulation and user-friendly interactions of CAD packages, as well as the advanced Additive Manufacturing (AM) technologies that transform complex CAD models into valid products. Among various theories and approaches for porous structure modeling in CAD, the unit cell method [4–6], [16] is one of the most broadly adopted. Armed with a library of primitive cell structures and automatic assembly strategies [5], [6], unit cell methods provide a powerful tool for both 2D and 3D porous structure modeling [23]. However, these methods are hampered by their poor capacities to exhibit pore diversity both in size and morphology. Alternative to unit cell methods, a set of reconstruction methods are proposed to mimic the porous structure in nature or construct irregular porous structures [10], [14], [21], [30]. The advantage of these reconstructed methods is that diverse pore shapes with non-uniform distribution can be constructed. However, these methods require that existing porous models must be at hand, which significantly restricts their applicability and efficacy.

To solve the aforementioned problems, Kou and Tan [20] proposed a simple but effective geometric representation for irregular porous structures based on stochastic Voronoi tessellation (VT). The key advantage of their method is that it generates irregular porous artifacts and no exiting media (e.g. MRI-based models) are called for. This method was further extended to represent irregular porous structures with graded pore sizes and distributions [19]. Despite that their methods enjoy much efficacy in constructing irregular porous structures on a global level; these methods lack the abilities to precisely control the local pore size and distribution since the Voronoi generators are randomly distributed during the process of porous structure modeling. Another disadvantage of their methods is that the obtained porous structures may not be effectively analyzed by

CONTACT S.T. Tan sttan@hkucc.hk

using either conventional finite element methods (e.g. finite element methods relying on triangular or tetrahedral meshes) or Voronoi cell finite element methods (VCFEMs) [11], [22]. By using the former ones, a large number of elements are always needed to accurately formulate the physical behavior of porous structures, leading to tremendous computational costs [2], [28]; by using the latter ones, ill-condition stiffness matrix and simulation errors will be introduced for the overly large or small angles within each Voronoi cell of porous structures [27].

Motivated to tackle these issues, we propose a new approach for irregular porous structure modeling. In this method, we apply centroidal Voronoi tessellation (CVT) rather than VT to control the pore size and distribution, and B-Spline to control the pore shape. In the remaining of this paper, we introduce the definition of CVT and the algorithm details of the CVT-based porous structure modeling strategy in Section2. In Section 3, three case studies are provided to demonstrate the efficacy of the proposed method in constructing irregular porous structures. The superiorities of our method to existing VT-based methods are also discussed. In section 4, a summary of this paper is drawn.

2. Porous structure modeling strategy

The proposed approach for irregular porous structure modeling mainly includes two steps: domain partition by CVT, and porous structure generation.

2.1. Domain partition by CVT

Centroidal Voronoi tessellations (CVTs) are Voronoi tessellations (VTs) of a region that their generating points coincide with the centroids of the corresponding Voronoi regions [8]. In the literature, VTs and CVTs have been greatly utilized to partition geometric domains and generate polygonal meshes [9], [29].

Given an open bounded domain $\Omega \in \Re^d$and a set of distinct points $\{\mathbf{x}_i\}_{i=1}^n$belong to Ω, for each point $\mathbf{x}_i$, the corresponding Voronoi region V_i consists of all the points in Ω that are closer to $\mathbf{x}_i$than to any other point in the set, i.e.:

$$V_i = \{\mathbf{x} \in \Omega || \mathbf{x} - \mathbf{x}_i| < |\mathbf{x} - \mathbf{x}_j| \quad \text{for } j = 1, \ldots, n \text{ and } j \neq i\} \tag{1}$$

where $|\cdot|$ denotes the Euclidean distance in $\Re^d$. We refer to$\{V_i\}_{i=1}^n$ as the VT of Ω and the points $\{\mathbf{x}_i\}_{i=1}^n$ as the associated generating points.

Given a density function $\rho(\mathbf{x})$ which is positive on Ω, for any region $V \subset \Omega$, we define $\mathbf{x}^*$, the centroid of V by

$$\mathbf{x}^* = \frac{\int_V \mathbf{x}\rho(\mathbf{x})d\mathbf{x}}{\int_V \rho(\mathbf{x})d\mathbf{x}} \tag{2}$$

A VT of Ω, $\{(\mathbf{x}_i, V_i)\}_{i=1}^n$, is called as CVT if and only if the generating points $\{\mathbf{x}_i\}_{i=1}^n$ associated with the Voronoi regions $\{V_i\}_{i=1}^n$ are also the centroids of those regions, i.e., if and only if $\mathbf{x}_i = \mathbf{x}_i^*$ for $i = 1, \ldots, n$. One common method to construct CVT is the Lloyd method. The construction process mainly includes four steps [8]:

(i) *Select an initial set of n points* $\{\mathbf{x}_i\}_{i=1}^n$ *on* Ω *according to the density function* $\rho(\mathbf{x})$*;*
(ii) *Construct the Voronoi regions* $\{V_i\}_{i=1}^n$ *of* Ω *corresponding to* $\{\mathbf{x}_i\}_{i=1}^n$*;*
(iii) *Compute the centroids of the Voronoi regions* $\{V_i\}_{i=1}^n$ *and use them to form the new set of points* $\{\mathbf{x}_i\}_{i=1}^n$*;*
(iv) *If the new points meet the stipulated criteria, return* $\{(\mathbf{x}_i, V_i)\}_{i=1}^n$*; otherwise, go to step (ii).*

As an example, Fig. 1. shows a VT and a CVT in a unit square with respect to a uniform density function $\rho(\mathbf{x}) = 1$. We can notice that the generating points (the red dots) of the CVT are more uniformly distributed than those of the VT.

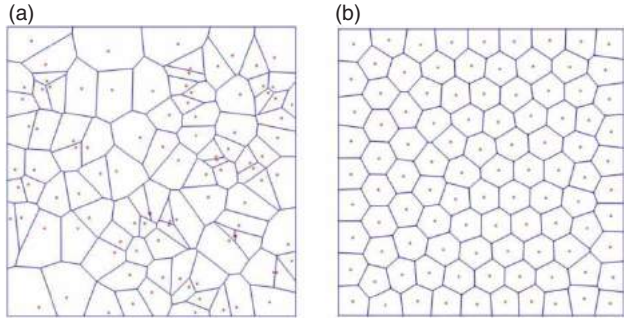

Figure 1. Voronoi tessellations on a unit square. (a) the general VT with uniformly distributed generating points; (b) the CVT derived from the general VT.

2.2. Porous structure generation

After constructing a CVT over the domain of interest, the porous structure is then generated by adding a pore into each Voronoi cell. The generation process of the porous structure in our method is similar to those in conventional methods based on VT [19], [20], except that we use CVT instead of VT. For the sake of simplicity, we give a brief introduction of the construction process of

the porous structure in what follows. Interesting readers may refer to [19], [20] for a comprehensive study.

Fig. 2. shows how a pore is built in a single Voronoi cell. Give an arbitrary Voronoi cell V_1, a scaled Voronoi cell is first generated according to the expression as below:

$$\mathbf{z}_{si} = \mathbf{z}_c + t(\mathbf{z}_i - \mathbf{z}_c),\ 0 < t \leq 1 \tag{3}$$

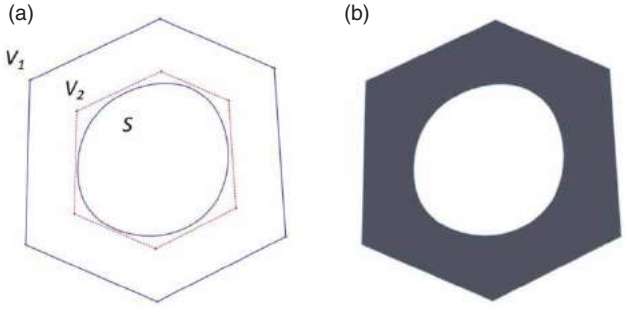

Figure 2. The construction process of a pore within a single Voronoi cell. (a) construct a B-Spline curve with the vertices of the scaled Voronoi cell being the control points; (b) generate the pore by using Boolean operations.

where $\mathbf{z}_i$ denotes the ith vertex in V_1, $\mathbf{z}_{si}$ denotes the corresponding vertex in the scaled Voronoi cell V_2, $\mathbf{z}_c$ denotes the centroid of V_1, and t is a scaling factor. A B-Spline curve S is then generated with the vertices of V_2 being the control points. Boolean difference is finally conducted between the Voronoi cell, V_1, and the area enclosed by the B-Spline curve, S, generating a porous Voronoi cell (see Fig. 2(b).).

It is worth mentioning that the scale factor t is used to control the pore size within each Voronoi cell. By setting different scale factors, various porous structures can be easily constructed on a given CVT. For instance, Fig. 3. shows two porous structure generated from the CVT depicted in Fig. 1(b). with the scale factor t being 0.8 and 0.6, respectively. In Fig. 3., the pore distribution is controlled by a uniform density function. Given a non-uniform density function, our method can easily construct irregular porous structure with non-uniform pore distribution, as shown in Fig. 4.

3. Implementation details

We have implemented the proposed method successfully in SolidWorks on various geometries. In this section, three case studies are presented to demonstrate the efficiency of the proposed algorithm in constructing irregular porous structures. The advantages of our method over existing VT-based methods are discussed.

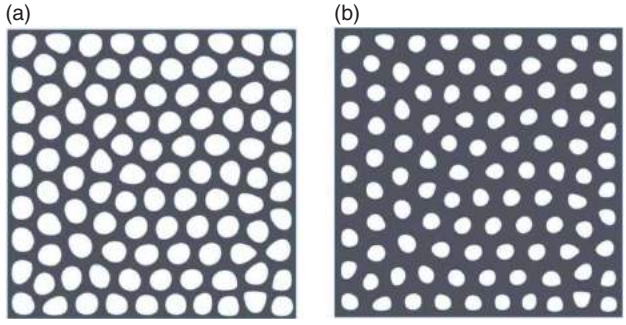

Figure 3. Uniform porous structures with different scale factors. (a) $\rho = 1, t = 0.8$; (b) $\rho = 1, t = 0.6$.

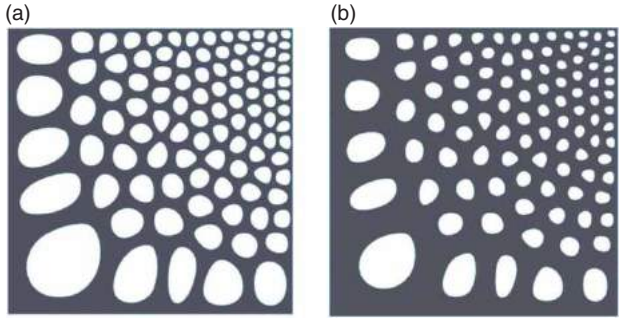

Figure 4. Non-uniform porous structures with different scale factors. (a) $\rho = x^2y^2, t = 0.8$; (b) $\rho = x^2y^2, t = 0.6$.

3.1. Case study 1: porous structure modeling on a unit circle

In the first case study, we set the domain of interest as a unit circle, i.e.

$$\Omega = \{(x,\ y)|x^2 + y^2 \leq 1\} \tag{4}$$

and we set the density function of CVT as an exponential function, i.e.

$$\rho(x,\ y) = e^{-10.0\sqrt{x^2+y^2}} \tag{5}$$

Fig. 5. shows the VT- and CVT-based porous structures with the scaling factor $t = 0.8$. Here the VT and CVT (the blue skeletons) are generated according to the same density function, i.e. Eqn. (5). The histogram on the left of the porous structure represents the distribution of angles within Voronoi cells of the VT and CVT.

3.2. Case study 2: porous structure modeling on a super ellipse

In the second case study, we study the porous structure modeling on a super ellipse which is defined as

$$\Omega = \{(x,\ y)|(x^4 + y^4)^{0.25} \leq 1\} \tag{6}$$

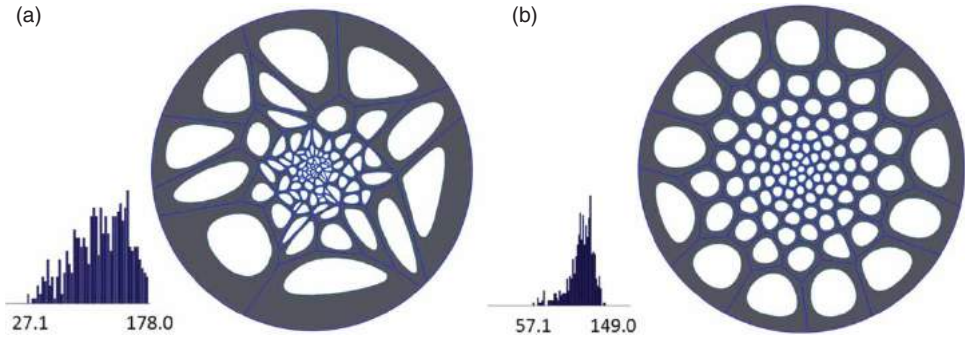

Figure 5. Irregular porous structures in the case study 1 with the scaling factor t being 0.8. (a) the VT-based porous structure; (b) the CVT-based porous structure.

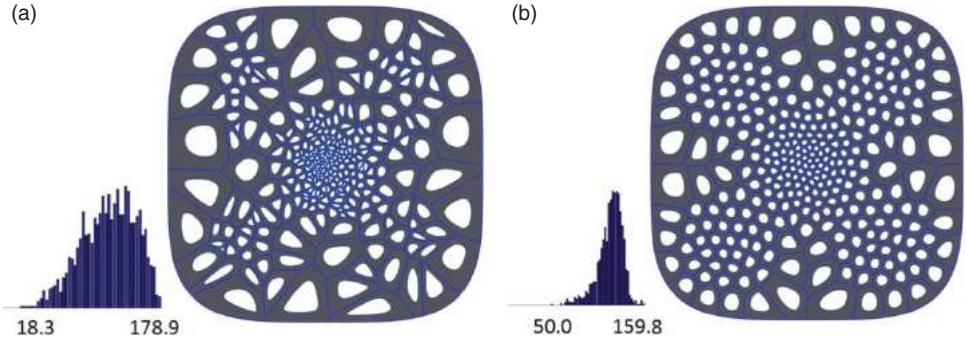

Figure 6. Irregular porous structures in the case study 2 with the scaling factor t being 0.6. (a) the VT-based porous structure; (b) the CVT-based porous structure.

and we set the density function as

$$\rho(x,\ y) = e^{-20.0(x^2+y^2)} + 0.1(\sin(\pi x)\sin(\pi y))^2 \quad (7)$$

Fig. 6. shows the VT- and CVT-based porous structures with the scaling factor $t = 0.6$.

3.3. Case study 3: porous structure modeling on an arbitrary domain

Different from the two case studies above, the domain of interest in the case study 3 is bounded by an arbitrary parametric curve (see Fig. 7.). In this case study, we set the density function as:

$$\rho(x,\ y) = (d(x,\ y))^3 \quad (8)$$

where $d(x,\ y)$denotes the distance from an arbitrary point $(x,\ y)$to the outer boundary. Fig. 7. shows the VT- and CVT-based the porous structures with the scaling factor $t = 0.5$.

From the three case studies described above, we can notice that our method can generate diverse porous structures on different kinds of geometries, either

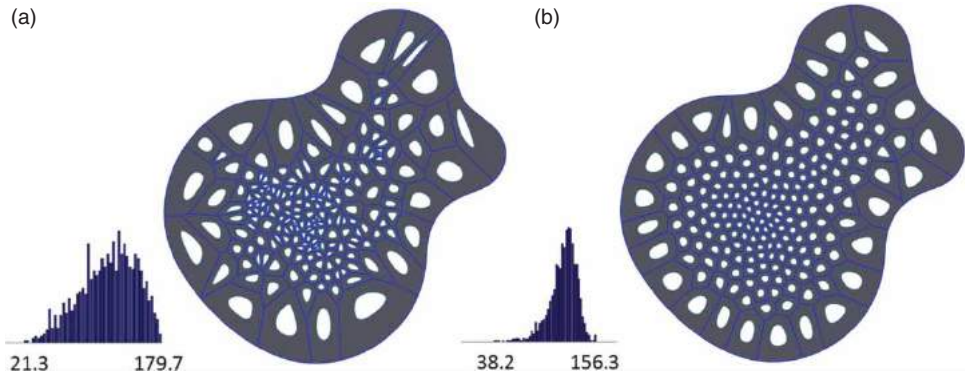

Figure 7. Irregular porous structures in the case study 3 with the scaling factor t being 0.5. (a) the VT-based porous structure; (b) the CVT-based porous structure.

implicit or parametric. We can also find that the pore size in the VT-based porous structure is distributed according to the given density functions globally, yet, the pore distribution is not exactly in accordance with the density functions locally. In the CVT-based porous structure, however, the pore size is distributed literally according to the given density functions, both globally and locally. As a result, our method demonstrates better performance on local control of pore size and distribution. In addition, from the histograms depicted in Fig. 5., Fig. 6., and Fig. 7., we can see that our method can significantly improve the quality of the polygonal mesh (VT or CVT) related to the porous structure, and avoid overly small or large angles which are very dangerous in finite element analysis (FEA) [27]. For example, in case study 1, the minimum angle (57.1°) within Voronoi cells of the CVT-based porous structure is larger than that of the VT-based porous structure (27.1°), while the maximum angle (149.0°) is smaller than that of the VT-based porous structure (178.0°).

4. Conclusion

In this paper, a new method for porous structure modeling based on CVT and B-Spline is introduced. Due to CVTs' superior properties, the proposed method generates porous structures with irregular pore shape, and diverse pore size and distribution according to a given density function. Compared to existing methods for porous structure modeling based on VT or Quadtree (Octree) [18], our approach are much more flexible to control the pore size and distribution both globally and locally. In addition, our method can significantly improve the quality of the polygonal mesh embedded into the porous structure, and avoid overly large or small angles which will influence the stiffness matrix conditions and simulation results in FEA [27].

Due to the advantages mentioned above, one potential application of the proposed method is that designers can utilize our CVT-based method to efficiently design optimized porous solids with respect to given requirements, such as strength and weight. The reason is that effective finite element simulations can be conducted on our CVT-based porous solids without tremendous computational costs and simulation errors. In addition, it is flexible to modify the underlying porous structures both globally and locally by changing the density functions of CVTs. And it has been proved that it is not hard to derive a density function from an estimator of FEA results [17]. Comprehensive investigations of such an application are beyond the scope of this paper and will be tackled in the future.

One weakness of this paper, however, is that 3D porous structure modeling is not taken into account. The reason is that constructing 3D CVT-based porous structures will always be a non-trivial task. For example, it is difficult to construct a 3D CVT with a set of generating points given in 3D space. It is also not easy to construct a B-Spline surface within a 3D CVT cell. In the future, we will extend the CVT-based method to 3D porous structure modeling.

Acknowledgement

The authors would like to thank the Department of Mechanical Engineering, the University of Hong Kong, and the Research Grant Council of Hong Kong SAR Government for their financial support.

ORCID

Y.H. You http://orcid.org/0000-0001-7069-2944

References

[1] Ajdari, A.; Nayeb-Hashemi, H.; Vaziri, A.: Dynamic crushing and energy absorption of regular, irregular and functionally graded cellular structures, International Journal of Solids and Structures, 48(3–4), 2011, 506–516. http://dx.doi.org/10.1016/j.ijsolstr.2010.10.018.

[2] Akanji, L.T.; Matthai, S.K.: Finite Element-Based Characterization of Pore-Scale Geometry and Its Impact on Fluid Flow, Transport in Porous Media, 81(2), 2010, 241–259. http://dx.doi.org/10.1007/s11242-009-9400-7.

[3] Barrios, M.; Van Sciver, S.W.: Thermal conductivity of rigid foam insulations for aerospace vehicles, Cryogenics, 55–56, 2013, 12–19.

[4] Chantarapanich, N.; Puttawibul, P.; Sucharitpwatskul, S.; Jeamwatthanachai, P.; Inglam, S.; Sitthiseripratip, K.: Scaffold library for tissue engineering: A geometric evaluation, Computational and Mathematical Methods in Medicine, 2012, 2012, 1–14.

[5] Chua, C.K.; Leong, K.F.; Cheah, C.M.; Chua, S.W.: Development of a tissue engineering scaffold structure library for rapid prototyping. Part 1: Investigation and classification, International Journal of Advanced Manufacturing Technology, 21(4), 2003, 291–301.

[6] Chua, C.K.; Leong, K.F.; Cheah, C.M.; Chua, S.W.: Development of a tissue engineering scaffold structure library for rapid prototyping. Part 2: Parametric library and assembly program, International Journal of Advanced Manufacturing Technology, 21(4), 2003, 302–312.

[7] Crupi, V.; Epasto, G.; Guglielmino, E.: Comparison of aluminum sandwiches for lightweight ship structures: Honeycomb vs. foam, Marine Structures, 30(0), 2013, 74–96. http://dx.doi.org/10.1016/j.marstruc.2012.11.002.

[8] Du, Q.; Faber, V.; Gunzburger, M.: Centroidal Voronoi tessellations: Applications and algorithms, Siam Review, 41(4), 1999, 637–676. http://dx.doi.org/10.1137/S0036144599352836.

[9] Du, Q.; Gunzburger, M.; Ju, L.L.: Advances in Studies and Applications of Centroidal Voronoi Tessellations, Numerical Mathematics-Theory Methods and Applications, 3(2), 2010, 119–142. http://dx.doi.org/10.1.1.407.3228.

[10] Feinberg, S.E.; Hollister, S.J.; Halloran, J.W.; Chu, T.M.G.; Krebsbach, P.H.: Image-based biomimetic approach to reconstruction of the temporomandibular joint, Cells Tissues Organs, 169(3), 2001, 309–321. http://dx.doi.org/10.1159/000047896.

[11] Ghosh, S.; Lee, K.; Raghavan, P.: A multi-level computational model for multi-scale damage analysis in composite and porous materials, International Journal of Solids and Structures, 38(14), 2001, 2335–2385. http://dx.doi.org/10.1016/S0020-7683(00)00167-0.

[12] Giannitelli, S.M.; Accoto, D.; Trombetta, M.; Rainer, A.: Current trends in the design of scaffolds for computer-aided tissue engineering, Acta Biomaterialia, 10(2), 2014, 580–594. http://dx.doi.org/10.1016/j.actbio.2013.10.024.

[13] Gibson, L.J.; Ashby, M.F.: Cellular solids: structure and properties, Cambridge University Press, 1997.

[14] Hollister, S.J.; Maddox, R.D.; Taboas, J.M.: Optimal design and fabrication of scaffolds to mimic tissue properties and satisfy biological constraints, Biomaterials, 23(20), 2002, 4095–4103. http://dx.doi.org/10.1016/S0142-9612(02)00148-5.

[15] Huber, O.; Klaus, H.: Cellular composites in lightweight sandwich applications, Materials Letters, 63(13–14), 2009, 1117–1120. http://dx.doi.org/10.1016/j.matlet.2008.11.059.

[16] Jang, W.Y.; Kraynik, A.M.; Kyriakides, S.: On the microstructure of open-cell foams and its effect on elastic properties, International Journal of Solids and Structures, 45(7–8), 2008, 1845–1875. http://dx.doi.org/10.1016/j.ijsolstr.2007.10.008.

[17] Ju, L.L.; Gunzburger, M.; Zhao, W.D.: Adaptive finite element methods for elliptic PDEs based on conforming centroidal Voronoi-Delaunay triangulations, Siam Journal on Scientific Computing, 28(6), 2006, 2023–2053. http://dx.doi.org/10.1137/050643568.

[18] Kou, S.; Tan, S.: An Approach of Irregular Porous Structure Modeling Based on Subdivision and NURBS, Computer-Aided Design and Applications, 10(2), 2013, 355–369. http://dx.doi.org/10.3722/cadaps.2013.355-369.

[19] Kou, X.Y.; Tan, S.T.: Microstructural modelling of functionally graded materials using stochastic Voronoi diagram and B-Spline representations, International Journal of Computer Integrated Manufacturing, 25(2), 2012, 177–188. http://dx.doi.org/10.1080/0951192X.2011.627948.

[20] Kou, X.Y.; Tan, S.T.: A simple and effective geometric representation for irregular porous structure modeling, CAD Computer Aided Design, 42(10), 2010, 930–941. http://dx.doi.org/10.1016/j.cad.2010.06.006.

[21] Mohebi, A.; Fieguth, P.; Ioannidis, M.A.: Statistical fusion of two-scale images of porous media, Advances in Water Resources, 32(11), 2009, 1567–1579. http://dx.doi.org/10.1016/j.advwatres.2009.08.005.

[22] Moorthy, S.; Ghosh, S.: A model for analysis of arbitrary composite and porous microstructures with Voronoi cell finite elements, International journal for numerical methods in engineering, 39(14), 1996, 2363–2398.

[23] Naing, M.W.; Chua, C.K.; Leong, K.F.; Wang, Y.: Fabrication of customized scaffolds using computer-aided design and rapid prototyping techniques, Rapid Prototyping Journal, 11(4), 2005, 249–259. http://dx.doi.org/10.1108/13552540510612938.

[24] Poulikakos, D.; Boomsma, K.: On the effective thermal conductivity of a three-dimensionally structured fluid-saturated metal foam, International Journal of Heat and Mass Transfer, 44(4), 2001, 827–836.

[25] Raj, S.V.: Microstructural characterization of metal foams: An examination of the applicability of the theoretical models for modeling foams, Materials Science and Engineering: A, 528(15), 2011, 5289–5295. http://dx.doi.org/10.1016/j.msea.2011.02.005.

[26] Scheffler, M.; Colombo, P.: Cellular Ceramics: Structure, Manufacturing, Properties and Applications, Wiley, 2005.

[27] Shewchuk, J.R.: What Is a Good Linear Element? Interpolation, Conditioning, and Quality Measures in Proceedings of the 11th International Meshing Roundtable, Sandia National Laboratories, 2002.

[28] Talebi, H.; Silani, M.; Bordas, S.P.A.; Kerfriden, P.; Rabczuk, T.: A computational library for multiscale modeling of material failure, Computational Mechanics, 53(5), 2014, 1047–1071. http://dx.doi.org/10.1007/s00466-013-0948-2.

[29] Talischi, C.; Paulino, G.H.; Pereira, A.; Menezes, I.F.M.: Polygonal finite elements for topology optimization: A unifying paradigm, International Journal for Numerical Methods in Engineering, 82(6), 2010, 671–698. http://dx.doi.org/10.1002/nme.2763.

[30] Tsakiroglou, C.D.; Ioannidis, M.A.; Amirtharaj, E.; Vizika, O.: A new approach for the characterization of the pore structure of dual porosity rocks, Chemical Engineering Science, 64(5), 2009, 847–859. http://dx.doi.org/10.1016/j.ces.2008.10.046.